



## OPEN ACCESS

## EDITED BY

Hao Liang,  
Sun Yat-sen University, China

## REVIEWED BY

Pengcheng Wang,  
Ocean University of China, China  
Linlin Li,  
School of Earth Sciences and  
Engineering, Sun Yat-sen University,  
China

## \*CORRESPONDENCE

Jiao Zhou,  
✉ 464946523@qq.com

## SPECIALTY SECTION

This article was submitted to  
Geohazards and Georisks,  
a section of the journal  
Frontiers in Earth Science

RECEIVED 08 August 2022

ACCEPTED 02 December 2022

PUBLISHED 23 January 2023

## CITATION

Zhou J, Chen H, Chen J, Yi S, Guo L,  
Hu X, Du W and Sun M (2023),  
Characteristics and distribution of  
geohazards since the middle miocene  
of the Xisha sea area, South China Sea.  
*Front. Earth Sci.* 10:1012144.  
doi: 10.3389/feart.2022.1012144

## COPYRIGHT

© 2023 Zhou, Chen, Chen, Yi, Guo, Hu,  
Du and Sun. This is an open-access  
article distributed under the terms of the  
[Creative Commons Attribution License  
\(CC BY\)](https://creativecommons.org/licenses/by/4.0/). The use, distribution or  
reproduction in other forums is  
permitted, provided the original  
author(s) and the copyright owner(s) are  
credited and that the original  
publication in this journal is cited, in  
accordance with accepted academic  
practice. No use, distribution or  
reproduction is permitted which does  
not comply with these terms.

# Characteristics and distribution of geohazards since the middle miocene of the Xisha sea area, South China Sea

Jiao Zhou<sup>1,2,3\*</sup>, Hongjun Chen<sup>1,2,3</sup>, Jiale Chen<sup>1,3</sup>, Shantang Yi<sup>1,3</sup>,  
Lihua Guo<sup>1,3</sup>, Xiaosan Hu<sup>1,2,3</sup>, Wenbo Du<sup>1,2,3</sup> and Meijing Sun<sup>1,2,3</sup>

<sup>1</sup>Key Laboratory of Marine Mineral Resources, Ministry of Natural Resources, Guangzhou Marine Geological Survey, China Geological Survey, Guangzhou, China, <sup>2</sup>Key Special Project for Introduced Talents Team of Southern Marine Science and Engineering Guangdong Laboratory, Guangzhou, China, <sup>3</sup>National Engineering Research Center for Gas Hydrate Exploration and Development, Guangzhou, China

Geological hazards can cause significant harm to the construction and maintenance of reef infrastructure projects in the Xisha Sea area. This study uses high-resolution multichannel earthquake data, single-channel seismic profiles, and multi-beam survey data to identify and analyze the geological hazards in the Xisha Sea area since the Miocene. Based on the geophysical data interpretation, the destructive geological disaster factors that are active, such as active faults, shallow gas, diapirs, landslides, multistage scarps (steps), scouring troughs, and canyons, as well as the restrictive geological disaster factors without activity ability, such as buried paleochannels, pockmarks, reefs, and undersea volcanoes, are identified and analyzed. This paper discusses the causes and hazards of geological hazards and, for the first time, draws a comprehensive plane layout of the geological hazards. The above analysis demonstrates that the scarps are mainly located around the atolls or platforms, and the slope of the southeast seabed topography is significantly higher than that of the northwest. There are seven medium and large landslides, mainly located around Yongxing Plateau and Yongle Plateau, caused by gravity and faulting. Shallow gas is mainly developed in the southern part of the North Reef and is indicated by diaper structures, faults, and gas chimneys. A series of shallow faults are developed in the study area, mainly steep normal faults. The scouring troughs are primarily distributed near the Yongxing Platform, Zhongjian North Platform, and Huaguang Platform. Submarine canyons are primarily located in the northern and southern parts of the Shidao Platform. Affected by multiple factors such as hydrodynamic conditions, the stability of sedimentary layers, and sediment supply, the scour degree varies, with the general depth ranging from several meters to several hundred meters. Underwater infrastructure in the study area should not be constructed in areas with active and destructive geological hazards. The results of this study can serve as a guide for further exploration in the Xisha area and disaster prevention and mitigation during construction activity in the area.

## KEYWORDS

Xisha sea area, high-resolution seismic, geological hazards, seabed scarps, submarine landslides, scour trough, spatial distribution

## 1 Introduction

Hazardous geology refers to naturally occurring or man-made geological conditions/phenomena that cause or can cause harm to human life or property. The research objectives of hazardous geological studies are the factors causing geological disasters, including geological bodies and geological phenomena and their occurrence, development mechanisms, and distribution (Liu et al., 2002). With the vigorous development of resource surveys in marine environments, such as for oil and gas, natural gas hydrate, and other marine engineering operations, the demand for a census of marine geological hazards has also been increasing. Marine disaster geology has also been continuously applied in practice, becoming a powerful means for achieving disaster prevention and mitigation in marine development activities (Bao and Jiang, 1993). In recent years, the instability of seabed geological conditions and the frequent occurrence of various marine disasters have increasingly affected human activities and economies (Ni, 2009; Li, 2013; Ma et al., 2014).

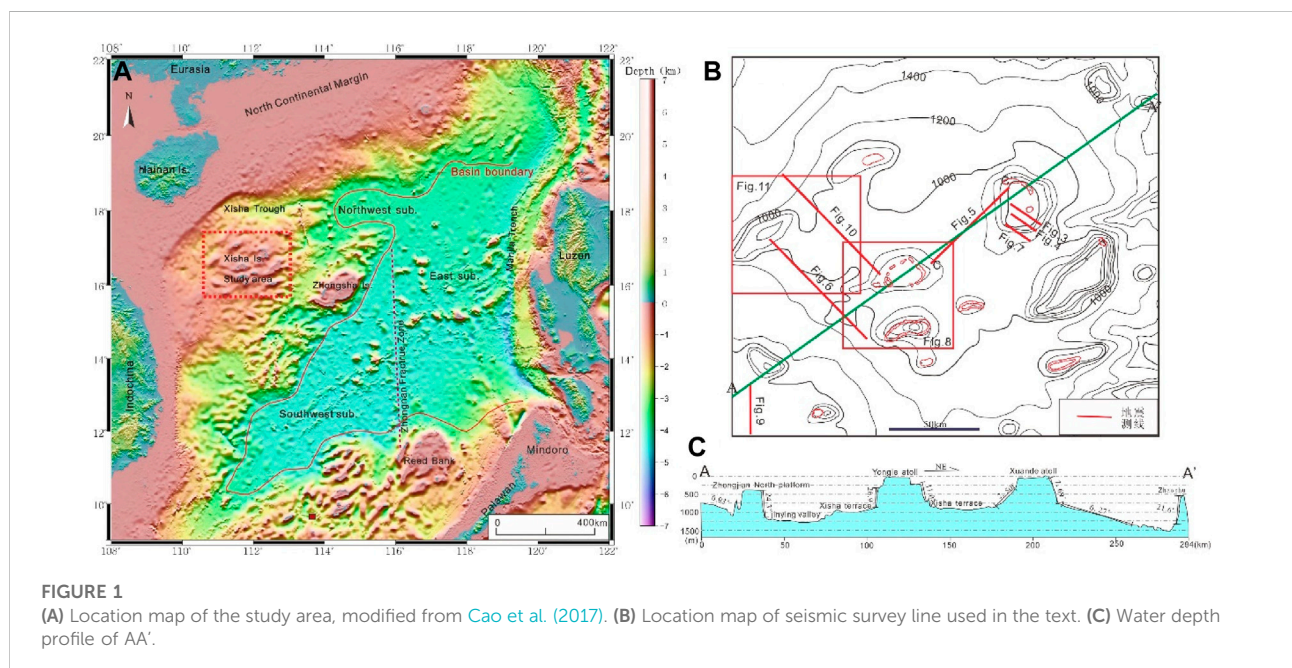
The South China Sea is located at the intersection of the Eurasian, Pacific, and Indo-Australian tectonic plates. The Xisha Islands are located northwest of the South China Sea (Figure 1). More than 40 islands, sandbars, reefs, and beaches are distributed in this sea. With a total island area of 8 km<sup>2</sup>, the Xisha Islands are the archipelago with the largest total land area among the four major archipelagos in the South China Sea. The development of infrastructure in the Paracel Islands and the development of industries such as the fishery and tourism industries have been essential to safeguarding national sovereignty. In recent years, the construction of Sansha City has been carried out rapidly.

Determining geological engineering conditions is crucial to ensure proper site selection and the safe construction of various projects. With the development, management, and promotion of tourism, fisheries, and seabed resources in the Xisha Islands, close attention must be paid to the possible risks of marine geological disasters affecting marine engineering facilities and the marine environment.

From the perspective of disaster-causing factors and disaster-laden environments, China's sea area is divided into four levels of geological disaster risk (Ye et al., 2011). Among them, the Xisha waters in the South China Sea belong to the land slope (island slope) disaster geological area (III<sub>3</sub>), a high-risk designation. There are few studies on the disaster geology of the Xisha sea area. Chen et al. (2021) studied the types and distribution characteristics of the disaster geology in the southeast of the Xuande Atoll in the Xisha Sea area. However, the research scope was small and with limitations. Using geophysical data collected since 2015, this paper comprehensively studied the types of geological disasters in the Xisha sea area and explored the causes of geological hazards. It is critical to fill the research gap, provide a basis for further exploration and disaster prevention and reduction to avoid the hazards in engineering construction, and provide a guarantee for particular navigation.

## 2 Geological setting

The South China Sea is located at the Indo-Australian Plate, the Eurasian Plate, and the Pacific Plate. It is the largest marginal sea basin in the Western Pacific and is part of the Western Pacific marginal trench-arc-basin system. The formation of continental



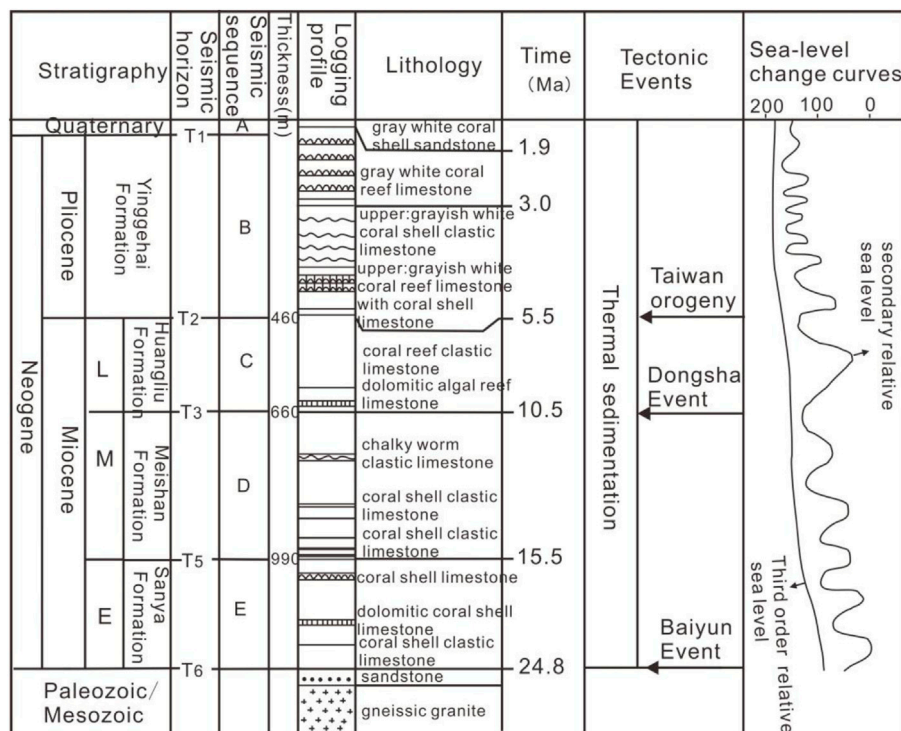


FIGURE 2

The stratigraphic column of XY1 well in the Xisha Sea area (Modified from Ma et al. (2010)).

margin basins in the northern part of the South China Sea is mainly related to the South China Sea movement and the Dongsha movement. It has undergone three stages: rifting, rifting with thermal subsidence, and the Cenozoic tectonic activity period (Kuang et al., 2014; Yang et al., 2016). The study area is located in the western part of the continental shelf and slope transition zone of the passive continental margin in the north of the South China Sea (Figure 1). It is adjacent to the continental shelf of Hainan Island in the west, the Xisha Trough in the north, and the Zhongsha Trough and South China Sea Basin in the East and south, respectively. The terrain is complex and changeable, mainly composed of islands, reefs, platforms, and valleys with a water depth of 0–2600 m.

The Xisha Sea area has experienced two tectonic evolution stages, the Paleogene fault depression, and the Neogene depression. It has a double-layer structure of a lower fault and upper depression, correspondingly forming two tectonic layers. The Xisha uplift area was in a state of uplift and denudation before the Miocene. Since the Miocene and the thermal subsidence of the South China Sea, the Xisha Sea area has sunk underwater and entered a period of large-scale reef formation. Reef formation has occurred in the area for more than 20 million years, and at present, reef facies sediments with a thickness of more than 1,200 m are present (He and Zhang, 1986; Lv et al., 2002; Lv et al., 2011; Yang et al., 2016). In the Xisha Sea

area, the drilling data of Well XY1 shows that since the Miocene, a vast reef formation developed on the Precambrian granite basement, reaching 1,251 m in thickness (Gong and Li, 1997; Zhao, 2010). Drilling data show that the entire area of the Xisha Islands subsided underwater since the Miocene, making the area have a suitable temperature, salinity, and water depth for the widespread development of reef carbonate formations.

The sequence stratigraphic framework since the Miocene in the study area has been established based on geophysical and drilling data (He and Zhang, 1986; Ma et al., 2010). Five third-order sequence interfaces (T<sub>1</sub>, T<sub>2</sub>, T<sub>3</sub>, T<sub>5</sub>, and T<sub>6</sub> (Figure 2)) are identified, which correspond to the bottom boundaries of the Quaternary, Pliocene, Late Miocene, Middle Miocene, and Early Miocene, respectively.

### 3 Materials and methods

Since 2015, the Guangzhou Marine Geological Survey has carried out 3,988 km of high-resolution single-channel seismic surveys, 1,205.7 km of multichannel seismic surveys, and 15,467 km of multi-beam bathymetry surveys in the Xisha Sea area (16°N–17°N, 111°E–112°30'E). The survey work has led to identifying the types and distributions of the geological hazards in the Xisha Sea area.

The single-channel seismic measurement used the IXSEA DELPH SEISMIC single-channel data acquisition and processing system. The seismic source adopted a GI gun source system, with a working pressure of 2000 psi and a capacity of 210. The SURESHOT source gun control system was used; the cable sinking depth was 0.5–1.5 m, and the subsidence depth of the source was 3 m. The offset distance between the GI air gun source and the receiving cable was 8–10 m. The length of the collected data record was 1000 m, and the width of the printed simulation profile was 400 m. In the muddy sedimentary area with a water depth of more than 30 m, the detection depth can reach (vertically) >100 m, and the vertical resolution was better than 3 m; under normal circumstances, the continuous missed test was less than 250 m, and the cumulative missed test was less than 6% of the entire survey line.

The shallow formation profile measurement used the EdgeTech3200XS CHIRP type shallow formation profiler. The recorded formation reflection signal was coherent and clear, and the formation reflection interface layer was clear and easy to trace continuously. The penetration depth in the work area reached ~30 m. The penetration depth could exceed 80 m.

The multichannel seismic measurement source system was composed of three rows of sub-arrays with a capacity of 1270 cu. in. and a total capacity of 3810 cu. in. The air gun controller was the Bigshot air gun synchronization controller produced by the Real Time System Company in the United States. The air compressor was the JOY4 air compressor. The working pressure was 2000PSI. The receiving cable of the receiving system adopted a Sentinel 24-bit digital solid cable of the France Sercel company, and 360 solid cables were used during the operation. The SYS3 water bird control system and the 5011E export compass controlled the cable depth control system. It consisted of a depth gauge and a 5010-type depth gauge; the water depth in the survey area was shallow, and the maximum water depth was less than 1200 m. Therefore, the multichannel seismic measurement adopted a parameter system with a focal depth of 7 m, a capacity of 3810  $in^3$ , and a cable depth of 9 m. Most of the measuring lines have an accuracy of less than 0.5 m. The first-grade rate was 92.28%, the second-grade rate was 7.72%, and the self-assessment pass rate was 100%.

The SIMRAD EM710S multi-beam bathymetry system was used according to the requirements for tolerance in the “Ocean Multi-beam Measurement Regulations” (DZ/T 0292–2016); the time limit difference was 0.6 m when the water depth was less than 30 m. When the water depth was greater than 30 m, the limit difference was 2% of the water depth.

## 4 Types of hazardous geology

At present, the classification of geological disasters in China is not consistent. Based on the disaster location, they are classified into surface and underground types. They are then subdivided into

direct, potential, and direct obstacles (Li, 1990). They are also classified into lithospheric, atmospheric, hydrosphere, and biosphere, according to the different spheres that cause disasters (Liu et al., 1992). Some scholars have proposed the types of hydrodynamics, aerodynamics, soil mechanics, gravity, and tectonic stress according to the dynamics that cause geological disasters (Chen and Li, 1993). In addition, according to the activity of the disaster geological factors, scholars have divided geological disasters into two types: those with destructive capabilities and those without destructive capabilities (Feng et al., 1996; Liu, 1996).

Further, based on the location of the internal and external dynamic systems and geological disaster factors, some scholars have divided geological disasters into four types: structural, coastal, submarine, and shallow (Liu et al., 2000). The authors of this paper believe that the purpose of geological disaster classification is to directly classify the geological disasters and their degree of harm and to clarify which geological disasters can be prevented and which cannot be prevented and only avoided. Therefore, based on the interpretation results of geophysical survey data in this study, the geological disasters are divided into two categories (Table 1): active and destructive geological disasters, such as active faults, shallow gas, diapirs, landslides, steep ridges, scour troughs, etc. The second comprises inactive geological hazards, such as buried ancient river channels, pockmarks, volcanic structures, etc.

## 5 Characteristics, distribution, and causes of major geological hazards

According to previous investigations and research results, numerous volcanoes (Zhang BK. et al., 2014; Zhang et al., 2014b; Feng et al., 2017), normal faults (Lin et al., 2009; Yang et al., 2015; Du et al., 2021), reefs (Wei et al., 2008; Yang et al., 2011), etc. Have been developed in the Xisha Sea area since Pliocene, and scarps, landslides, faults, etc. (Chen et al., 2021) are developed in the southeast of Xuande Atoll, A large number of pits are developed near the Xisha Uplift area (Chen, 2011; Sun et al., 2012; Guan et al., 2014; Chen et al., 2015; Ye et al., 2019; Yang et al., 2020; Wang et al., 2021). Based on a large amount of new measured data, a large number of steep slopes, shallow gas, buried ancient river channels, large landslides, shallow faults, and scour channels have been newly discovered in this paper. The geological disasters in Xisha Islands have been systematically summarized for the first time. Landslides, steep slopes, shallow gas, mud diapirs, buried ancient river channels, shallow active faults, pits, scour channels, and other geological hazard phenomena are primarily located throughout the study area (Figure 3), which are potentially harmful to marine engineering. The following describes the main geological characteristics and the distribution of the geological hazards.



**FIGURE 3**  
Geological distribution map of environmental hazards in Xisha Sea area.

## 5.1 Destructive and active geological hazards

### 5.1.1 Multistage scarps (steps)

The seabed topography is mainly controlled by the Xisha platform and is closely related to the distribution of islands in the study area. The overall topography is characterized by islands at the center, declining altitude towards the surrounding area, with the upper slope being steep and the lower slope being gentler. The water depth ranges from 0 m to 800 m, and coral islands, reefs, and their subordinate platforms are developed throughout. The topographic variations of each island and reef are similar, characterized by a steep slope in the southeast and a gentle slope in the northwest. The average slope value of the periphery ranges between  $5.0^{\circ}$  and  $22.0^{\circ}$ . The distribution of landslide masses from north to south can reach  $30^{\circ}\text{km}$ , which is considerable. The water depth is less than 300 m, and the steep slope of the plateau changes violently, with a slope of about  $21^{\circ}$ . The plateau slope reduces within a water depth of 300–950 m with a slope value of about  $1.5^{\circ}$ .

The study area includes Yongle Atoll and Xuande Atoll, where many reefs and reef platform uplifts are developed. In many platform edges or steep areas, the coral reef strata grow in a cliff-like manner and go down the platform with a multi-level steep ridge (more than  $5.6^{\circ}$ – $10^{\circ}$ , Figure 4). The height difference ranges from hundreds of meters to kilometers, and there is a gradual downward slope reduction in the multi-level scarps. The scarps in the study area are primarily located at the edges of the Ganquan Platform, the China Construction Beihai Platform, the Yongxing Atoll, the Yongle Atoll, the Dongdao Platform, etc. The submarine topographic slope of the southeast side is significantly higher than that of the northwest side. The average submarine slope of the scarps on the northwest side of the island reef area is about  $4.6^{\circ}$ , and the average submarine slope of the scarps on the southeast side is about  $22^{\circ}$ . For example, the scarp in the southeast of Xuande Atoll (Figure 4) is a two-level scarp, of which the primary scarp has a gradient of  $7.8^{\circ}$  and an elevation of 416 m. The secondary scarp has a gradient of  $14.8^{\circ}$  and an elevation of 460 m.

The scarps in the study area are closely related to the development of the carbonate platform in the Xisha area.

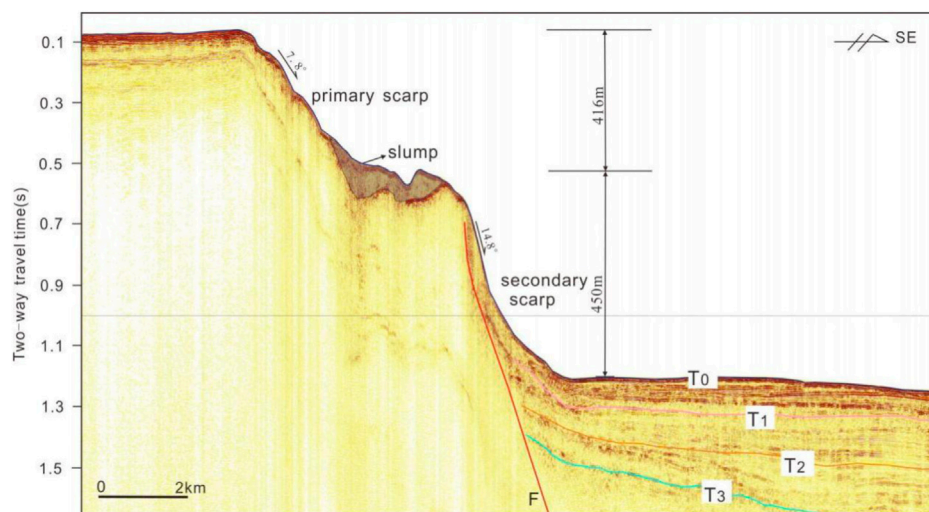


**FIGURE 4**

The reflection characteristics of stepped scarps and slumping deposits are shown on a single earthquake.

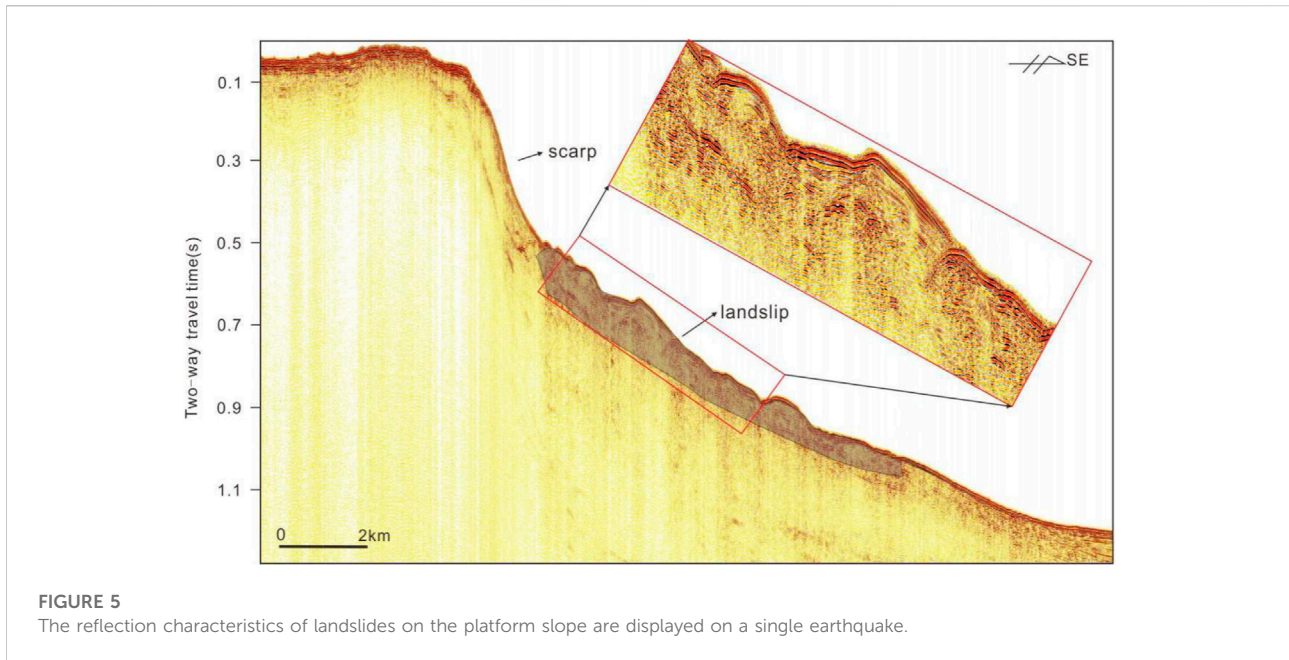
During the Middle Miocene, the sea level was relatively high, and the carbonate platform expanded vertically and horizontally. The slope basin around the platform gradually entered the semi-deep sea environment and began receiving numerous gravity flow sediments transported in turbidity currents. During the late Miocene, the relative sea level rose rapidly again, and the platform mainly grew longitudinally (Yang et al., 2014; 2016; Li et al., 2020). The platform as a whole deposited a thicker layer of carbonate rock strata, forming a large atoll reef several kilometers above the sea floor (Ma et al., 2011). This has resulted in the formation of many scarps and landslides. These scarps can cause erosion, fracture activity, landslides, and other effects and should be regarded as active, destructive geological hazards (Ma et al., 2017). Generally, the degree of soil consolidation in these scarps is poor, which makes them an adverse topographic factor when laying and maintaining submarine pipelines. They can also easily cause platform tilt and pipeline sliding (Liu et al., 2014).

### 5.1.2 Submarine collapse/landslide

A submarine landslide is a phenomenon in which unconsolidated soft sediments or rocks with weak structural planes on the sea floor move downward along a weak structural plane under gravity. It includes geological processes such as sliding, collapse, and debris flow (Hampton et al., 1996; Locat and Li, 2002; Moscardelli et al., 2006; Moscardelli and Wood, 2008; Wang Dawei et al., 2009, 2011; Wu et al., 2011). They also include mass transport deposits (MTDS).

Submarine collapses/landslides in the study area are related to local magmatic activities, faults, scarps, or steep slopes. Generally, they occur in areas with a particular drop in the

terrain, such as slope areas around a platform and the edges of seamounts (mounds). Due to their gravity, faults, and other factors, local sediments lose stability, slide down, and collapse along the slope or fault. They then pile up disorderly at places with flat terrain and open accommodation spaces on the platform slope, forming collapsed sedimentary bodies. This collapsing phenomenon in the study area is mainly distributed on the slopes around the platform, with irregular shapes or multiple mound-shaped reflections, internal chaotic reflections (Figure 5 and Figure 6), no stratification, and mainly reef debris accumulations. There are seven medium and large landslides identified in the study area, including two in the west and one in the southeast of Yongxing Plateau, two in the west and two in the south of Yongle Plateau, with an area of 323 km<sup>2</sup>, 100 km<sup>2</sup>, 176 km<sup>2</sup>, 116 km<sup>2</sup>, 96 km<sup>2</sup>, 173 km<sup>2</sup>, and 99 km<sup>2</sup>. Here, we take the large landslide with an area of 323 km<sup>2</sup> found on the west side of the Yongxing Plateau as an example (Figure 6), distributed within 500–950 m of water depth. The length of the landslide mass from north to south can reach 30 km, the maximum width is 13 km, and the cliff on the side wall of the landslide can reach 345 m. The seismic profile shows that the landslide comprises two parts: the slow accumulation landslide at the back end and the fast accumulation landslide at the front end, which was formed during the late Miocene. Multiple landslide surfaces are developed inside, indicating that the landslide is characterized by multistage and multistage development. There are many waterways and buried ancient rivers in the landslide body. The waterways are generally 700 m wide and 30 m deep, with an average gradient of 5.5°. Multistage secondary small landslides are widely developed on both sides of the waterways. The front rapid landslide body has chaotic



reflection seismic facies, reflecting the rapid accumulation of sediments. It is a typical submarine landslide fan. In addition, some submarine landslide valleys have not been filled by sediments, indicating that there was still activity during the Quaternary.

A landslide is very harmful to offshore engineering facilities. Due to its instability, it often leads to the collapse of offshore structures installed on it. This causes damage to offshore engineering facilities, such as deep-sea oil and gas drilling installations, oil pipelines, submarine cables, etc., leading to potential heavy casualties and economic losses. Submarine landslides can also cause huge waves and even tsunamis (Fine et al., 2005; Ni, 2009; Li, 2013).

### 5.1.3 Shallow gas

Shallow submarine gas usually refers to the gas accumulations in sediments less than 1,000 m below the sea floor (Davis, 1992). Shallow submarine gas is widely distributed throughout Chinese seaways. In some places, the oil and gas seedlings of the sea surfaces have a history of more than 100 years (He et al., 2000; He et al., 2010). Engineering hazards caused by shallow gas have also been reported frequently (Chen et al., 2010; Guo et al., 2013; Liu et al., 2019).

The interpretation of multichannel seismic data and the rich acoustic anomalies present in the data directly prove the existence of shallow gas in the study area. Seismic records show that the reflections between the layers of gas-bearing sediments are chaotic. The reflected waves with good continuity are suddenly interrupted, and the co-axial axis is hidden or disappears altogether, or the reflection is blurred. Further, the reflections are columnar, sac-like, and strip-like but not

rule-like. The southern part of the North Reef is mainly composed of shallow gas as indicated by diapir structures, faults, and gas chimneys (Figure 7A). Deep fluid or gas upwelling has occurred, part of which was captured by the Middle-Late Miocene reefs to form a reef trap (shown in the earthquake data as a tower tip mound reflection in the  $T_3$ - $T_5$  interface). Part of the gas continued upwelling to the shallow stratum, and some gas was even released into the seawater. This process caused the interruption of the horizontal axis in the stratum, forming chaotic reflections in the shape of columns, mushrooms, etc. The surrounding and upper sedimentary layers generated numerous strong reflections. The top surface is wavy, clearly defined with the surrounding rock, and has clear upward warping traction characteristics (Figure 7D). The bright spots and scattered reflections on the section indicate that gas played an essential role in the middle stage of the formation of this type of structure. The natural gas and fluid permeability are related to the formation of these uplifts or mud diapirs. BSR (Bottom Simulating Reflector) are seen in the upper strata of the mud diapirs and gas chimneys (Figure 7C), and a blank band appears above the BSR, indicating gas hydrate accumulation in the mud diapirs in the peripheral seafloor sediments. At the top of the gas chimneys and mud diapirs, many shallow minor faults control the upward leakage of shallow gas, forming gas chimneys, and there is a pull-down phenomenon in the same internal direction axis (Figure 7B).

### 5.1.4 Active fracture

Active faults are one of the hazard types that require great attention when it comes to offshore engineering. The geophysical

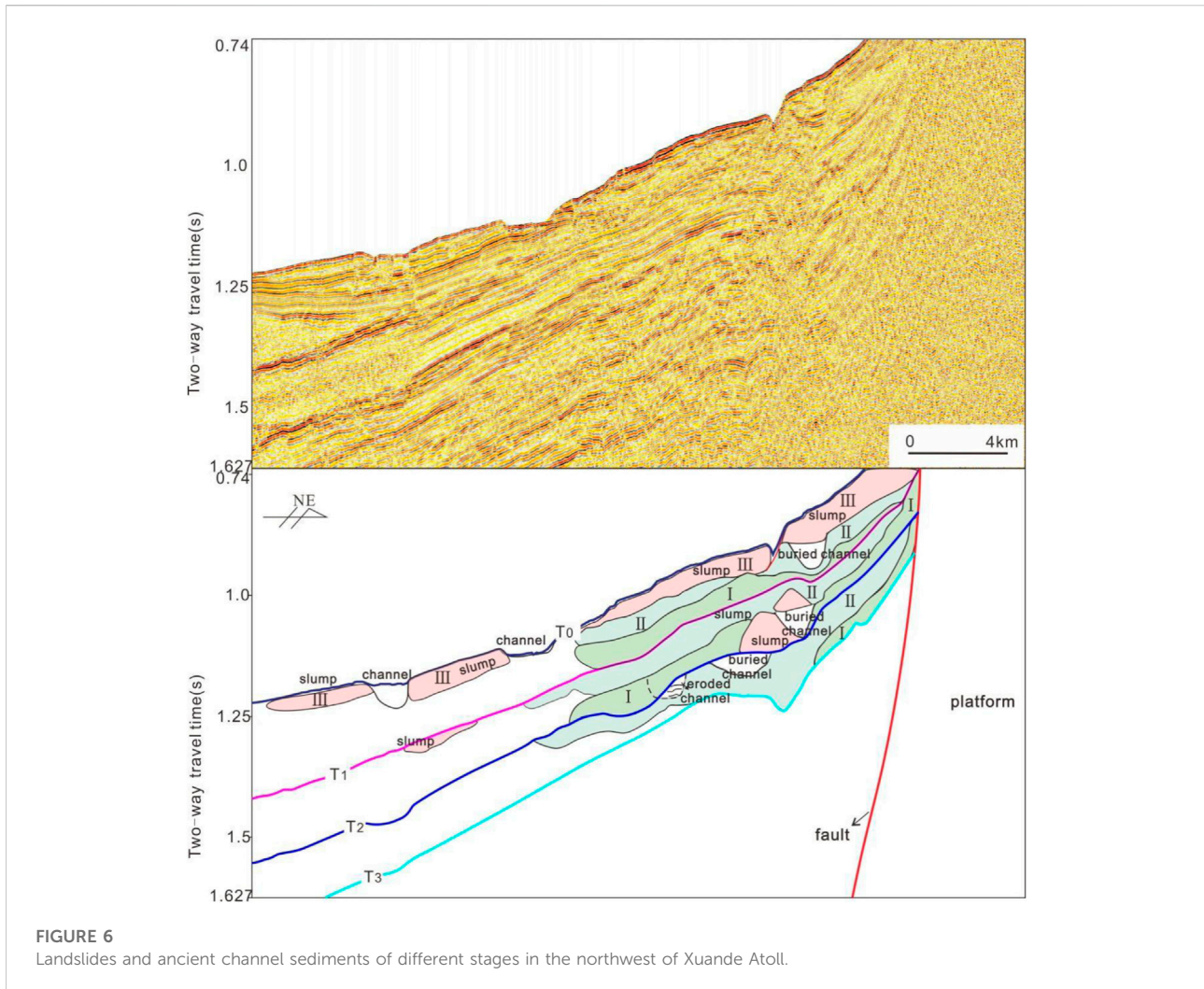


**FIGURE 6**  
Landslides and ancient channel sediments of different stages in the northwest of Xuande Atoll.

data and the geological background of the study area indicate that the shallow faults in the study area were still active in the Quaternary, making them potentially quite dangerous. Some of the detrimental effects of these faults include the fact that they may directly affect offshore engineering activities. For example, when the drilling activity encounters a fault, it may lead to a stuck pipe and mud leakage (Ma and Chen, 2006). The seismic activity and stratum collapse caused by secondary faults are potential geological hazards.

The formation of the Xisha block was mainly controlled by the surrounding fault structures and affected by the multistage expansion of the South China Sea basin, forming the tectonic evolution characteristics of a “lower fault and upper depression.” There are many deep and large faults on the platform’s periphery, such as the Xisha Trough fault zone and the Binhai fault zone on the north side, the Ailaoshan-Honghe fault zone on the west side, and the Zhongsha Trough fault zone on the south side (Xu et al., 2010; Cao et al., 2014). A

series of normal faults with extensional shear properties are developed along these fault zones (Lin et al., 2009), and a series of normal faults are also developed in the transition zone between the Xisha block and the northwest sub-basin, indicating that the area has prominent extensional characteristics (Ding et al., 2009).

Many small shallow faults are developed in the study area in NE-NEE and NW directions. They are also mainly normal faults with a steep occurrence, vertical fault displacement of about 10m, and horizontal fault displacement of less. They are staggered  $T_1$  (Quaternary stratigraphic bottom) seismic reflection interface and the seabed (Figure 11). In the single-channel seismic section, the faults are characterized by in-phase axis dislocation and distortion, different internal and external reflection patterns of the reflection wave groups on both sides of the fault, and sometimes an inconsistent thickness of the two plates. The faults are associated with volcanic activity, gas-bearing structures, and pockmarks.

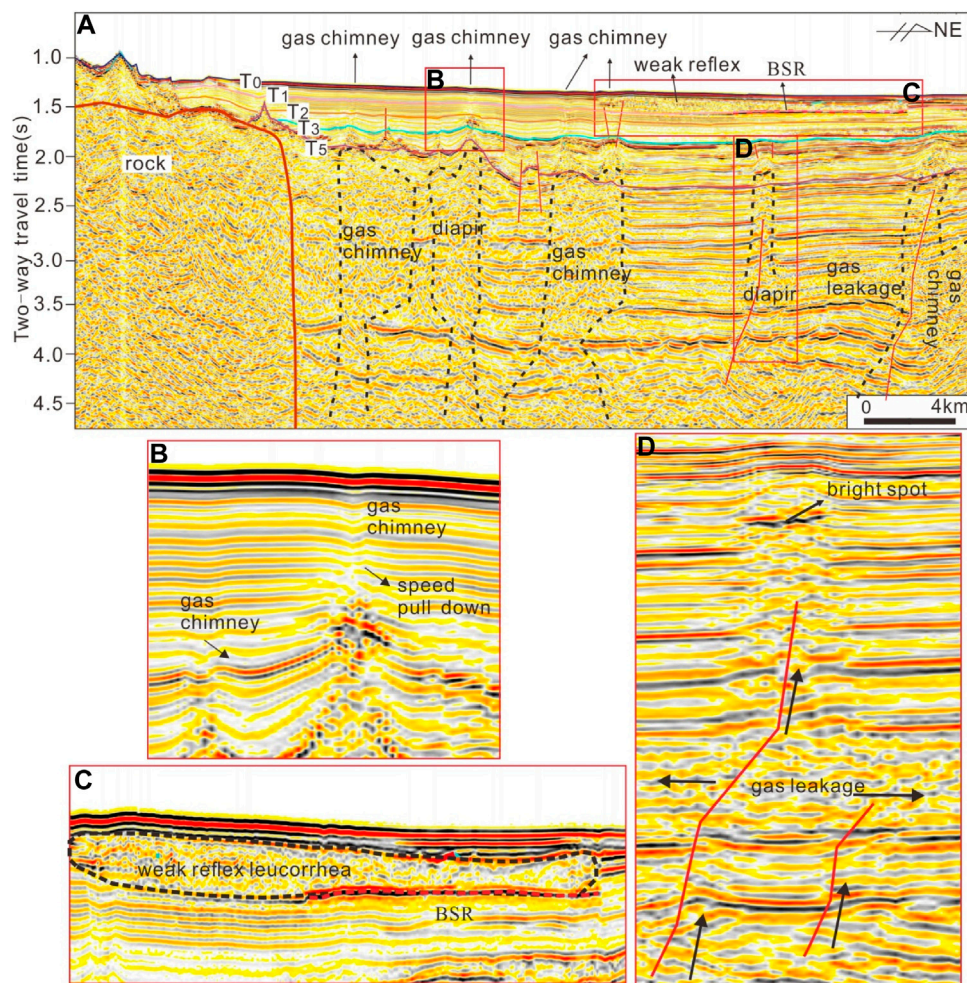


**FIGURE 7**

Schematic diagram of seismic profile of mud diapir and gas chimney at the edge of the platform (B). (C) and (D) are magnified views of corresponding parts in (A).

### 5.1.5 Submarine erosion of gullies (troughs) and canyons

Submarine scour gullies (troughs) are widely developed around the platforms. They are mainly distributed on the southern and eastern slopes of the Yongxing Platform, the southwest and southeast slopes of the Zhongjian North Platform, and the northwest and southern slopes of the Huaguang Platform (Figure 3). They are large or small and often occur in groups. The cross-section of the scour trough is mostly V-shaped and U-shaped, the wall of the valley side is relatively steep, and the sediments are collapsed (Figure 8), being controlled by the faults. Along the fault boundary, the sediments are continuously scoured by the current, denuded, and accumulate at the bottom of the valley for local deposition or transported and redeposited with the current. The current seafloor scour gullies have been affected by multiple factors,

such as hydrodynamic conditions, stability of the sediment layer, and sediment supply. The scour degree varies, with most water depths ranging from several meters to several hundred meters. On the southern side of the Xuande Platform in the study area, a series of east-west and north-south erosion grooves are developed on the slope (Figure 9). These grooves occur in water depths of 350 m–750 m; the cutting depth of the grooves ranges from 15 m to 40 m, and the width of the grooves mouths ranges from 110 m to 500 m. The grooves extend along the slope into deep water, nearly parallel to each other, forming a train of skirts around the reef.

There are more than six small and medium-sized canyons in the study area. The head of these small canyons generally has multiple branches and is connected with other geomorphic units, such as erosion and scouring grooves, which are in a “funnel” shape on the plane. The scales of these canyons are larger than

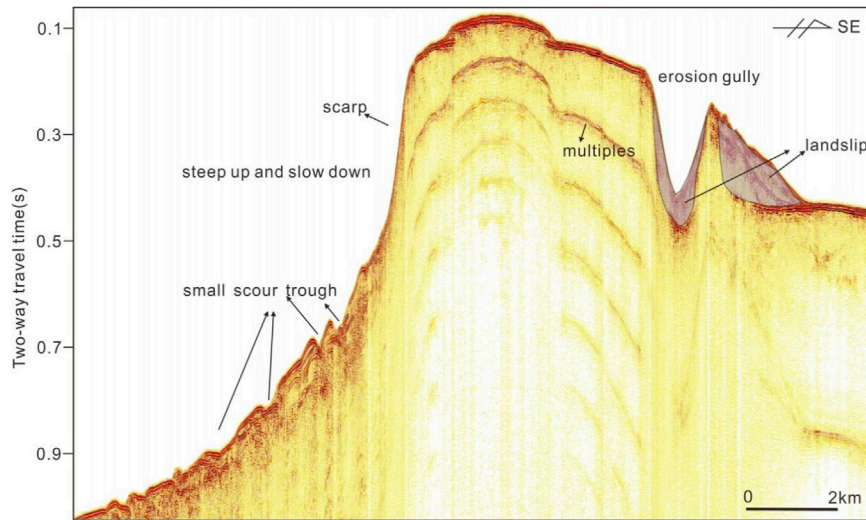


**FIGURE 8**  
Scour trough phenomenon reflected on a single earthquake.

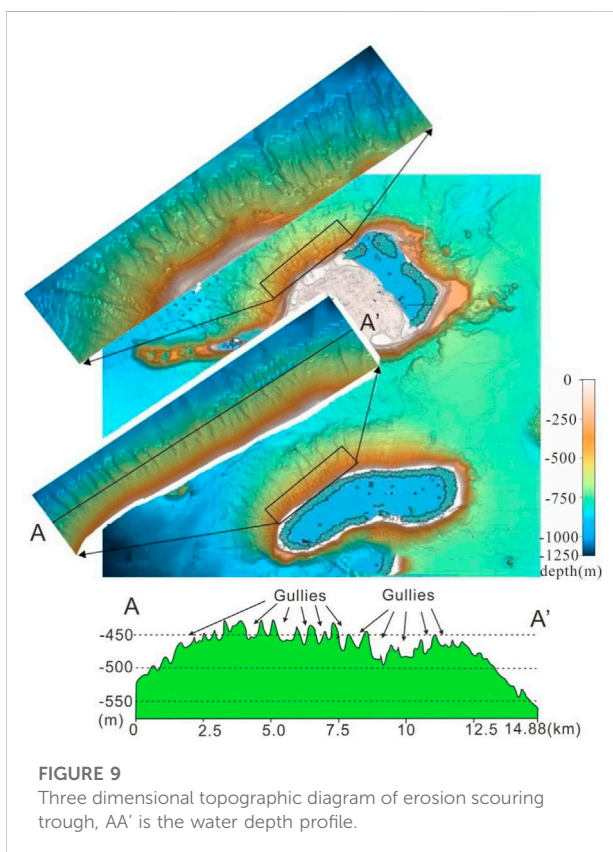


**FIGURE 9**  
Three dimensional topographic diagram of erosion scouring trough, AA' is the water depth profile.

that of steep slope erosion grooves, with a length of up to 20 km and a width of about 600 m–1500 m. The cross section of the canyons is V-shaped, and the undercutting erosion depth is

generally 20 m–40 m. Generally, the erosion depth of the upper half of the canyons is deep, and the undercutting erosion depth of some small canyons in the south of the Huaguang Plateau can reach 150 m. The most typical canyon is the Yongle Canyon, located north of the East Island Platform (Li et al., 2017). The overall morphology of the Yongle canyon is several small canyons on the northeast side of the East Island platform converging into the main big canyon leading to the northwest sub-basin. The upstream slope of the Yongle Canyon is steep and varies greatly, and the channels around the atoll and the submarine landslide system are the transport channels of detrital materials in the source region. In the middle and lower reaches of the basin, the slope is gentle, the slope variation is slight, and the detrital material is mainly transported and merges into the erosion and collapse debris on both sides of the slope, forming a horn-shaped entrance basin in the northwest sub-basin (Wu and Qin, 2009).

The canyon area and scour trough are continually affected by erosion, a typical active geological hazard. The terrain changes are complex, and the unstable sediments on both sides of the valley slopes and valley shoulders cause fracturing and distortion of pipelines in the area and dumping of the foundation piles of drilling platforms. Also, the topographic conditions on both sides of the eroded valley/canyon can cause the strata on both sides to be deposited. Collapse or slip can occur, causing devastating damage to various constructions around it. Therefore, areas with eroded valleys/canyons should be avoided when choosing sites for engineering activities. In particular, the eroded valleys south of the Xuande Atoll, the west and southeast of the Middle North Sea Platform, the northwest of the Huaguang Reef, and the canyons on the northern and southern sides of the Dongdao

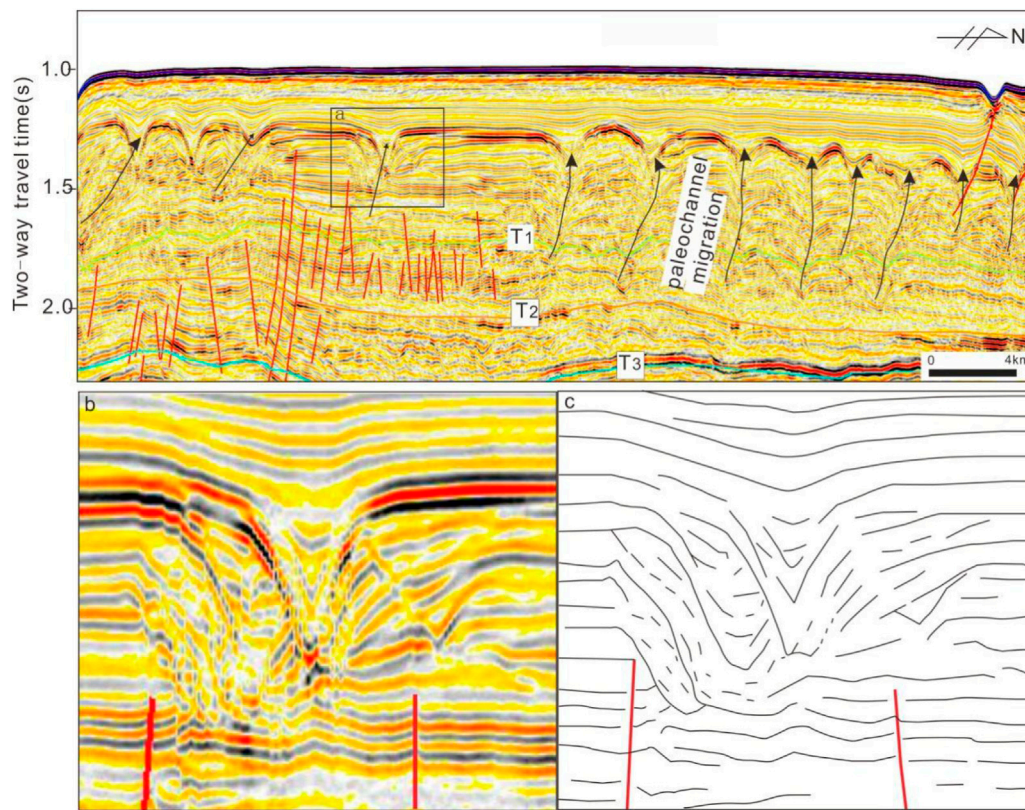


**FIGURE 10**  
Seismic profile of buried paleochannel migration, where (B) is the enlarged part of (A), (C) is the fine description of the internal structure of (B)

Platform should be avoided when looking to create underwater engineering structures.

## 5.2 Destructive and inactive geological hazards

### 5.2.1 Buried palaeochannels

During the Wurm glacial stage of the Late Pleistocene, the global sea level generally dropped, the sea water retreated, and the continental shelf was exposed to land. Rivers and lakes of various scales developed. Since the Holocene, with the sharp rise in the sea level, the early channels sunk into the seabed, and most were buried under sediments of different thicknesses, forming ancient buried channels.

The paleochannels in the study area mainly developed between the  $T_0$  to  $T_2$  interface in the sediments from the Late Pliocene to the Late Pleistocene with NW-trending and NE-trends. Figure 10 shows that 12 continuously migrating paleochannels developed in the southwest corner of the Xisha area. The paleochannels in different periods are crisscrossed

vertically and horizontally, superimposed on each other, and show complex variations. Wave-like reflection interfaces can be seen at the bottom of the paleochannels, and chaotic discontinuous-relatively continuous reflections reflect the strata inside the ancient rivers. It shows that the study area in the Late Pliocene-Late Pleistocene was in an erosion and scouring stage and went through many stages of erosion-filling-re-erosion-refilling.

Paleochannel sediments are often complex and variable, and physical and mechanical properties vary significantly in the horizontal direction, such as particle size composition, sorting degree, density, compressive strength, and shear strength. The sediments and fillings of the paleochannels are mainly coarse clastic sand and gravel with large porosity, fast interlayer water circulation, and strong permeability. These could have easily been generated by long-term erosion, scour, and overburden loads in the strata (Kou, 1990; Chen and Li, 1993; Bao, 1995). Local collapse destroys the formation's original structure and causes basement instability. River sediments often contain a large amount of organic matter, which may form shallow gas.

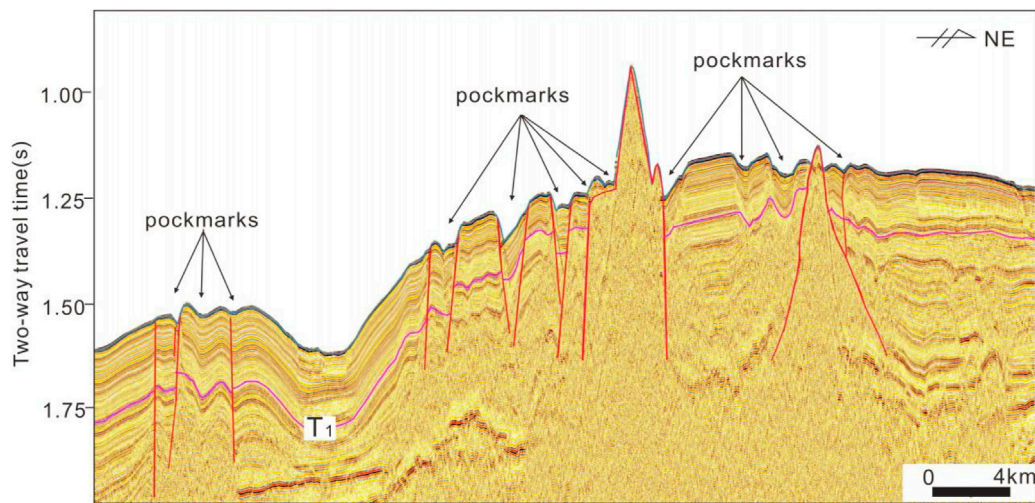


**FIGURE 11**  
Active faults and Markeng recorded by single seismic profile.

This gas makes the area unsuitable for constructing offshore pile foundations and drilling platforms.

### 5.2.2 Seabed pockmarks

Submarine pockmarks are a negative seafloor topography formed by fluid and gas in formations leaking upward along migration channels and eroding the sediments on the seabed surface (Judd et al., 2007; Hovland et al., 2012; Luo et al., 2012; Riboulot et al., 2013; Riboulot et al., 2014; Andreassen et al., 2017). The continued escape of gas from a formation can cause sediments to collapse, creating pits on the seafloor surface. The results of multi-beam surveys show that large and small pits in the study area are highly developed, especially on the northwest side, where the scales are large. Multiple pits are distributed together to form a pockmark group. Four larger pockmarks groups are located on the east side of the Ganquan Plateau, the south side of the Xisha Trough, the south side of the Jinyin Valley, and the southwest side of the Xuande Atoll. This paper temporarily named them the Ganquan East Pockmark Group, the Xisha Trough South Pockmark Group, the Valley South Pockmarks Group, and the Xuande South Pockmarks Group. The strata in the pockmarks area are mainly characterized by weak or scattered local reflections (Figure 11), and a large number of normal faults are developed in the shallow part.

The Ganquan East Pockmark Group is the largest one in the study area (Figure 12). It is dumbbell-shaped (wide on both sides and narrow in the middle), with an area of about 1505 km<sup>2</sup>. It is about 56.5 km long in the NS direction, 15–44 km wide in the EW direction, and has a water depth of 850–1250 m. There are three small pit groups arranged along

the NE direction in the Xisha Trough South Pockmark Group (with a total area of about 1409 km<sup>2</sup>), the westernmost of which is in the shape of a NE-direction strip, and the other two are irregular. The Valley South Pockmark Group is smaller, about 176.2 km<sup>2</sup>, and a small oval-shaped depression is developed on the west side of the group. It is ~2.4 km long, 1.3 km wide, and 3.2 km<sup>2</sup> in area. The water depth in the depression is about 120 m; The Xuande South Pockmarks Group is in the shape of an irregular strip and is about 22.5 km long, 3–4 km wide, and 72.8 km<sup>2</sup> in area. Several small sea mounds are developed in the pockmark group.

It is generally thought that deep fluids (such as hydrocarbon gas, pore fluid, groundwater, etc.) migrate upward to shallow formations through migration channels (such as faults, unconformities, weak zones, etc.) and accumulate to form overpressure formations. When the pressure of the overlying formation decreases and the overpressure fluid in the lower part breaks through the seal, the fluid leaks. At the same time, the pore water in the formation is discharged from the pore space and transported to the seabed sediments, causing the relatively weak local seabed sedimentary formations to deform. The pore water also gradually erodes the local seabed formations, reducing the volume of sediments and forming pits (King and Maclean, 1970; Harrington, 1985; Scanlon and Knebel, 1989; Khandriche and Werner, 1995; Cathles et al., 2010). The pits in the study area are mainly of tectonic origin and have been generated due to faults, gas chimneys, mud volcanoes, mud diapirs, and other tectonic processes related to fluid activities. The undulating seabed topography in the area of the pockmark groups and the uneven settlement inside and outside the pockmarks can adversely affect cables and pipelines

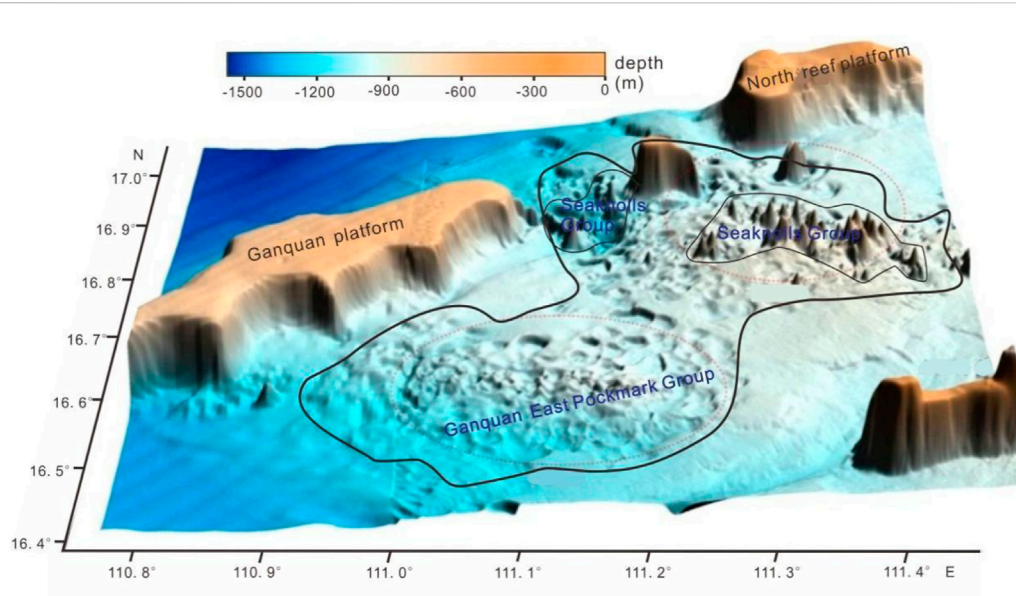


**FIGURE 12**  
Three-dimensional topographic map of the Ganquan East Pockmark Group and Seaknolls Group.

**TABLE 1 Geological classification of disasters in the Xisha Sea area.**

Geological hazard type	Geological hazard factors
Destructive geological hazards with activity ability	Active fault, shallow gas, diapir, landslide, scarp, scouring trough, canyon
Destructive geological hazards without activity capacity	Buried palaeochannels, pockmarks, bioherms, mounds, volcanic structures

laid in the area, and, therefore, doing so should be treated with caution.

### 5.2.3 Submarine volcanoes

Existing studies have pointed out that in the northwest of the South China Sea, where the Xisha Sea area is located, after seafloor expansion, volcanic structures with small individual areas, large numbers, and apparent inherited activity became widely distributed (Zhang et al., 2014b). There is a concentrated distribution of Cenozoic volcanic activity in the area (Zhang et al., 2014b). Seismic profiles show about 10 volcanic structures in the southern part of the Xisha Sea area (Feng et al., 2017). According to our latest data, about 30 volcanic structures intrude into the Quaternary strata in the Xisha Sea area, even erupting out of the sea floor to form seamounts with different sizes and exposed areas ranging from 1.5 km<sup>2</sup> to 125 km<sup>2</sup>. Volcanic structures are mainly manifested in the perforation of the seabed, typical low-frequency and strong reflections of the contour, internal chaos, discontinuous strong amplitude reflection characteristics or blank discontinuous weak reflection characteristics, and a main invasion of the Pliocene

and Pleistocene strata. In addition, a single volcanic structure has been found in the western edge, and central part of the Xisha area, and volcanic activity has invaded the surrounding Quaternary strata.

Active volcanoes have a strong disaster-causing effect, but most of the submarine volcanoes in the study area are no longer active, making them inactive geological hazards. The submarine volcanoes in the study area have had a noticeable transformation effect on the submarine topography, resulting in a considerable height difference between the volcanoes and the surrounding strata. The volcanoes have also dragged or disturbed the surrounding strata, resulting in the instability of the strata, making the area not conducive to laying large-scale pipelines or constructing platforms.

## 6 Conclusion

Based on the interpretation and analysis of geophysical data and from the perspective of geological hazards in the Xisha Sea area, the following conclusions are drawn:

- 1) Based on the interpretation of geophysical survey data, the geological hazards are divided into two categories: active and destructive geological hazards, such as active faults, shallow gas, diapirs, landslides, steep ridges, scour grooves, etc. The second comprises inactive geological hazards, such as buried ancient river channels, pits, etc.
- 2) The steep ridges are mainly located around the atolls or platforms. The average submarine slope of the scarps on the northwest side of the island reef area is about 4.6°, and the average submarine slope of the scarps on the southeast side is about 22°. Landslides are mainly developed in the west and southeast of the Yongxing Plateau and the west and south of the Yongle Plateau. There are seven medium and large slumps caused by gravity and faulting. Shallow gas is mainly developed in the southern part of the North Reef and mainly includes shallow gas indicated by diapirs, faults, and gas chimneys. The shallow faults in the study area are mainly steep normal faults. The paleochannels in the study area are mainly developed in the sediments of the Late Pliocene to the Late Pleistocene with NW and NE trends, and they underwent a multistage erosion-filling-re-erosion-refilling process. In the Xisha Sea area, there are four large pockmark groups, the Ganquan East Pockmark Group, the Xisha Trough South Pockmark Group, the Haigu South Pockmark Group, and the Xuande South Pockmark Group. They are mainly tectonic, including faults, gas chimneys, mud volcanoes, mud diapirs, and other structures related to fluid activities. Due to the influence of multiple factors, such as hydrodynamic conditions, the stability of sedimentary layers, and sediment supply, the scour valleys on the seafloor vary in terms of the scour degree. The degree of scouring varies from several meters to several hundred meters.
- 3) If engineering construction is to be carried out, hidden dangers should be identified before offshore construction, and measures should be taken to prevent harm to engineering infrastructure. To prevent geological disasters, engineering constructions should not be carried out in various shallow seabeds, especially active ones. Areas with geological hazards, such as the steep ridges around various atolls and platforms, landslides on the west and southeast sides of Yongxing Island, landslides in the west and south of Yongle Plateau, shallow gas in the southern part of the North Reef, active faults, mud diapirs, scour trough and canyon should be avoided when undertaking construction works in the area.

## References

- Andreassen, K., Hubbard, A., Winsborrow, M., Patton, H., Vadakkepuliambatta, S., Plaza-Faverola, A., et al. (2017). Massive blow-out craters formed by hydrate-controlled methane expulsion from the Arctic seafloor. *Science* 356 (6341), 948–953. [J]. doi:10.1126/science.aal4500
- Bao, C. W. (1995). Buried ancient channels and deltas in the continental shelf area of the Pearl River Estuary. *Mar. Geol. Quat. Geol.* 15 (2), 25–34.

## Data availability statement

The original contributions presented in the study are included in the article/supplementary material, further inquiries can be directed to the corresponding author.

## Author contributions

JZ, writing-original draft, review, editing, drawing. HC, writing-review and editing. JC, writing-Seismic profile interpretation. SY, writing-multibeam interpretation, methodology. LG, writing-drawing. XH, writing-multibeam interpretation and interpretation. WD, writing-review. MS, writing-review.

## Funding

This research was supported by the talent team introducing major special projects from the Guangdong Laboratory of Southern Marine Science and Engineering (Guangzhou) (GML2019ZD0201) and National Natural Science Foundation of China (91958212), the China Geological Survey Project (DD20221712, DD20221719, DD20190209, DD20190627).

## Conflict of interest

The authors declare that the research was conducted in the absence of any commercial or financial relationships that could be construed as a potential conflict of interest.

## Publisher's note

All claims expressed in this article are solely those of the authors and do not necessarily represent those of their affiliated organizations, or those of the publisher, the editors and the reviewers. Any product that may be evaluated in this article, or claim that may be made by its manufacturer, is not guaranteed or endorsed by the publisher.

Bao, C. W., and Jiang, Y. K. (1993). YK Types and characteristics of submarine potential geological hazards in China's offshore areas. *Tropical Ocean* 18 (3), 24–31.

Cao, J. H., Sun, J. L., Xu, H. L., and Xia, S. H. (2014). Seismological features of the littoral fault zone in the Pearl River Estuary. *Chin. J. Geophys.* 57 (2), 498–508.

- Cao, Y., Li, C. F., and Yao, Y. J. (2017). Thermal subsidence and sedimentary processes in the South China Sea Basin. *Marine Geology* 394, 30–38. doi:10.1016/j.margeo.2017.07.022
- Cathles, L. M., Su, Z., and Chen, D. F. (2010). The physics of gas chimney and pockmark formation, with implications for assessment of seafloor hazards and gas sequestration. *Mar. Petroleum Geol.* 27 (1), 82–91. doi:10.1016/j.marpetgeo.2009.09.010
- Chen, D. X., Wu, S. G., Wang, X. J., and Lv, F. (2011). Seismic expression of polygonal faults and its impact on fluid flow migration for gas hydrates formation in deep water of the South China Sea. *J. Geol. Res.* 2011, 1–7. doi:10.1155/2011/384785
- Chen, G. F., Chen, H. F., Hong, M., Guan, G. L., and Zhao, R. (2010). A brief discussion on the harm of harmful gases in Hangzhou Metro Tunnels and the prevention measures. *J. Railw. Eng.* 27 (5), 82–86.
- Chen, J. R., and Li, Y. H. (1993). Types and distribution of geological hazards in the South China Sea. *J. Geol.* 67 (1), 76–85.
- Chen, J. X., Guan, Y. X., Song, H. B., Yang, S. K., Geng, M. H., Bai, Y., et al. (2015). Distribution characteristics and geological implications of pockmarks and mud volcanoes in the northern and Western continental margins of the South China Sea. *Chin. J. Geophys.* 58 (3), 919–938. doi:10.6038/cjg20150319
- Chen, M., Xia, Z., Liu, W. T., He, J., and Ma, S. Z. (2021). Geohazards characteristics in the southeast of Xuande atoll, Xisha, south China sea. *J. Trop. Oceanogr.*. Available At: <https://kns.cnki.net/kcms/detail/44.1500.P.20210630.1525.004.html>.
- A. M. Davis (Editor) (1992). "Methane in marine sediments," 12, 1075–1264. *Cont. Shelf Res.* 10
- Ding, W. W., Li, M. B., Zhao, L. H., Ruan, A. G., and Wu, Z. L. (2009). Cenozoic tectono-sedimentary characteristics and extension model of the northwest sub-basin, south China sea. *Earth Sci. Front.* 16 (4), 147–156. [J].
- Du, W. B., Cai, G. Q., Huang, W. K., Chen, J. L., Nie, X., and Wang, X. M. (2021). Seismic reflection characteristics of Neogene carbonate platforms in the Xisha Sea area and their controlling factors. *Mar. Geol. Front.* 37 (1), 20–30.
- Feng, Y. C., Zhan, W. H., Sun, J., Yao, Y. T., Guo, L., and Chen, M. (2017). The formation mechanism and characteristics of volcanoes in the Xisha waters since Pliocene. *J. Trop. Oceanogr.* 36 (3), 73–79.
- Feng, Z. Q., Feng, W. K., Xue, W. J., Liu, Z. H., Chen, J. R., Li, W. F., et al. (1996). *Geological hazards and submarine engineering geological conditions in the northern South China Sea*. Nanjing, China: Hehai University Press, 10–100. [M].
- Fine, I. V., Rabinovich, A. B., Bornhold, B. D., Thomson, R. E., and Kulikov, E. A. (2005). The Grand Banks landslide-generated tsunami of November 18, 1929; preliminary analysis and numerical modeling. *Mar. Geol.* 215, 45–57. doi:10.1016/j.margeo.2004.11.007
- Gong, Z. S., and Li, S. T. (1997). *Analysis of continental margin basins and hydrocarbon accumulation in the northern South China Sea*. Beijing, China: Science Press, 10–70. [M].
- Guan, Y. X., Luo, M., Chen, L. Y., Wang, S. H., Yan, W., Wang, H. B., et al. (2014). Tracer study on the activity of submarine giant pits in the Western South China Sea. *Geochemistry* 43 (6), 628–639.
- Guo, A. G., Kong, L. W., Shen, L. C., Zhang, J. R., Wang, Y., Qin, J. S., et al. (2013). Study on the prevention and control measures of shallow gas hazard in subway construction. *Geotech. Mech.* 34 (3), 769.
- Hampton, M. A., Lee, H. J., and Locat, J. (1996). Submarine landslides. *Rev. Geophys.* 34 (1), 33–59. doi:10.1029/95rg03287
- Harrington, P. K. (1985). Formation of pockmarks by pore-water escape. *Geo-Marine Lett.* 5, 193–197. doi:10.1007/bf02281638
- He, J. X., Li, M. X., and Huang, B. J. (2000). Distribution of oil and gas seedlings and analysis of oil and gas exploration prospects in the northern slope of Yinggehai basin. *Nat. Gas. Geosci.* 11 (2), 1–9.
- He, J. X., Zhu, Y. H., Weng, R. N., and Cui, S. S. (2010). Characters of north— West mud diapirs volcanoes in south China sea and relationship between them and accumulation and migration of oil and gas. *Earth Science—Journal China Univ. Geosciences* 35 (1), 75–86.
- He, Q. X., and Zhang, M. S. (1986). *Xisha reef facies geology in China*. Beijing: Science Press, 1–182. [M].
- Hovland, M., Jensen, S., and Indreiten, T. (2012). Unit pockmarks associated with lophelia coral reefs off mid-Norway: More evidence of control by 'fertilizing' bottom currents. *Geo-Mar. Lett.* 32 (5–6), 545–554. doi:10.1007/s00367-012-0284-0
- Judd, A. G., and Hovland, M. (2007). *Seabed fluid flow: The impact of geology biology and the marine environment*. Cambridge, UK: Cambridge Univ Press. [M].
- Khandriche, A., and Werner, F. (1995). "Freshwater induced pockmarks in bay of eckernfoerde, western baltic[C]/Mojski JE," in Proceedings of the 3rd Marine Geological Conf, The Baltic (Warszawa: Prace Panstwowego Instytutu Geologicznego), 155–164.
- King, L. H., and Maclean, B. (1970). Pockmarks on the scotian shelf. *Geol. Soc. Am. Bull.* 81, 3141–3148. doi:10.1130/0016-7606(1970)81[3141:potss]2.0.co;2
- Kou, Y. Q. (1990). Paleochannel and its engineering geological evaluation of the northern continental shelf of the South China Sea. *Mar. Geol. Quat. Geol.* 10 (1), 37–45.
- Kuang, Z. G., Guo, Y. Q., Wang, L. L., Liang, J. Q., and Sha, Z. B. (2014). Discovery and evolution of late Miocene atoll system in Xisha Sea area. *Chin. Science:Earth Sci.* 44 (12), 2675–2688.
- Li, F. (1990). *Institute of oceanography, Chinese academy of Sciences marine science series (31 episodes)*. Beijing, China: Ocean Press, 25–49. [A]//Study on disastrous geology in the west of the South China Sea
- Li, Q., Wang, X., Ao, M., Gabrielson, E., Askin, F., Zhang, H., et al. (2013). Aberrant Mucin5B expression in lung adenocarcinomas detected by iTRAQ labeling quantitative proteomics and immunohistochemistry. *Clin. Proteomics* 6, 15–21. doi:10.1186/1559-0275-10-15
- Li, X. J., Wang, D. W., Wu, S. G., Wang, W. W., and Liu, G. (2017). Geomorphology of Sansha canyon: Identification and implication. *Mar. Geol. Quat. Geol.* 37 (3), 28–36.
- Li, X. L., Zhang, H. Y., Liu, G., Han, X. H., Qin, Y. P., and Wu, S. G. (2020). Seismic and evolution model of isolated carbonate platform-A case from Yongle Atoll, Xisha Islands. *Mar. Geol. Quat. Geol.* 40 (5), 87–96.
- Lin, C. S., Tang, Y., and Tan, Y. H. (2009). Geodynamic mechanism of dextral strike-slip of the Western-edge faults of the South China Sea[J]. *Acta Oceanol. Sin.* 31 (1), 159–167.
- Liu, L. J., Fu, M. Z., Li, J. G., Li, X. S., Chen, Y. N., Gao, S., et al. (2014). Geologic hazards in the deep pipeline routing area of the Liwan 3-1 gas field in the South China Sea[J]. *Adv. Mar. Sci.* 32 (2), 162–174.
- Liu, S. Q., Liu, X. Q., Wang, S. J., and Guo, Y. G. (2002). Discussion on some problems in compilation of hazardous geological map (1:2000000) of South China Sea. *Chin. J. Geol. Hazard. Control* 13 (1), 17–20.
- Liu, Y. X., Zhan, W. H., and Lu, C. B. (1992). types, laws and Prevention Countermeasures of geological disasters along the coast of South China. *Trop. Ocean.* 11 (2), 46–53.
- Liu, Z. H. (1996). *Feng Zhiqiang, Feng Wenke, Xue Wanjun, et al. Geological hazards and submarine engineering geological conditions in the northern South China Sea*. Nanjing, China: Hehai University Press, 2–95. [M].Types and characteristics of potential geological disasters
- Liu, Z. Y., Han, Z., Su, B., Ma, Y. F., and Li, Y. G. (2019). Characteristics of harmful gases in shallow layer of subway engineering and advanced exhaust measures. *J. Undergr. Space Eng.* 15 (S1), 479–485.
- Locat, J., and Lee, H. J. (2002). Submarine landslides: Advances and challenges. *Can. Geotech. J.* 39 (1), 193–212. doi:10.1139/t01-089
- Luo, M., Wu, L. S., and Chen, D. F. (2012). Research status and progress of seabed pockmarks. *Mar. Geol. Front.* 28 (5), 33–42.
- Lv, B. Q., Xu, G. Q., Wang, H. G., and Zhao, H. M. (2002). sea floor spreading recorded by drowning events of cenozoic carbonate platforms in the South China sea. *Chin. J. Geol.* 37 (4), 405–414.
- Lv, C. L., Yao, Y. J., Wu, S. G., and Yao, G. S. (2011). Seismic responses and sedimentary characteristics of the Miocene wan'an carbonate platform in the southern south China sea. *Earth Science-Journal China Univ. Geosciences* 36 (5), 931–938.
- Ma, S. Z., and Chen, T. H. (2006). Marine geological hazards in the pearl river estuary. *Guangdong Geol.* 21 (4), 13–21.
- Ma, Y., Kong, L., Liang, Q. Y., Lin, J. Q., and Li, S. Z. (2017). Characteristics of hazardous geological factors on the Dongsha continental slope in the northern South China Sea. *Earth Sci. Front.* 24 (4), 102–111.
- Ma, Y., Li, S. Z., Xia, Z., Zhang, B. K., Wang, X. F., and Cheng, S. X. (2014). Characteristics of hazardous geological factors on shenhu continental slope in the northern south China sea. *Earth Science-Journal China Univ. Geosciences* 39 (9), 1364–1372.
- Ma, Y. B., Wu, S. G., Gu, M. F., Dong, D. D., Sun, Q. L., Lu, Y. T., et al. (2010). Seismic reflection characteristics and sedimentary model of carbonate platform in Xisha sea area. *J. Oceanogr. Ed.* 32 (4), 118–128.
- Ma, Y. B., Wu, S. G., Lv, F. L., Dongdong, D., Qiliang, S., Yintao, L., et al. (2011). Seismic characteristics and development of the Xisha carbonate platforms, northern margin of the South China Sea. *J. Asian Earth Sci.* 40, 770–783. doi:10.1016/j.jseas.2010.11.003
- Moscaredelli, L., Wood, L., and Mann, P. (2006). Mass-transport complexes and associated processes in the offshore area of Trinidad and Venezuela. *Am. Assoc. Pet. Geol. Bull.* 90 (710), 1059–1088. doi:10.1306/02210605052
- Moscaredelli, L., and Wood, L. (2008). New classification system for mass transport complexes in offshore Trinidad. *Basin Res.* 20 (1), 73–98. doi:10.1111/j.1365-2117.2007.00340.x

- Ni, D. (2009). Marine disasters and disaster reduction in the past decade. *Mar. Geol. Dyn.* 9, 96.
- Riboulot, V., Cattaneo, A., Sultan, N., Garziglia, S., Ker, S., Imbert, P., et al. (2013). Sea-level change and free gas occurrence influencing a submarine landslide and pockmark formation and distribution in deepwater Nigeria. *Earth Planet. Sci. Lett.* 375, 78–91. doi:10.1016/j.epsl.2013.05.013
- Riboulot, V., Thomas, Y., Berne, S., Jouet, G., and Cattaneo, A. (2014). Control of Quaternary sea-level changes on gas seeps. *Geophys. Res. Lett.* 41 (14), 4970–4977. doi:10.1002/2014gl060460
- Scanlon, K. M., and Knebel, H. J. (1989). Pockmarks in the floor of penobscot bay, Maine. *Geo-Marine Lett.* 9, 53–58. doi:10.1007/bf02262818
- Sun, Q. L., Wu, S. G., Cartwright, J., and Dong, D. (2012). Shallow gas and focused fluid flow systems in the pearl river mouth basin, northern south China sea. *Mar. Geol.* 315–318, 1–14. [J]. doi:10.1016/j.marpetgeo.2012.05.003
- Wang, L., Wang, B., Li, J., Yu, K. Q., and Zhao, F. (2021). Morphology characteristics and formation mechanisms of submarine pockmarks in the northern Zhongjiannan Basin, South China Sea. *J. Trop. Oceanogr.* 40 (5), 71–84.
- Wei, X., Jia, C. Z., Meng, W. G., Zhu, Y. J., and Zhang, J. F. (2008). Discussion on the distribution of reefs and the direction of oil and gas exploration in the Xisha Sea area since Neogene. *Pet. Geophys. Explor.* 43 (3), 308–312.
- Wu, S. G., and Qin, Y. S. (2009). The research of deepwater depositional system in the northern South China Sea. *Acta Sedimentol. sin.* 27 (5), 922–930.
- Xu, H. L., Ye, C. M., Qiu, X. L., Sun, J. L., and Xia, S. H. (2010). Studies on the Binhai fault zone in the northern south China sea by the deep geophysical exploration and its seismogenic structure. *South China J. Seismol.* 30 (S), 10–18.
- Yang, S. X., Qiu, Y., and Zhu, B. D. (2015). *Atlas of geology and geophysics of the South China sea*. Tianjin, China: China Navigation Publications Press. [M].
- Yang, T. T., Lv, F. L., Wang, B., Fan, G. Z., Wang, X., Lu, Y. T., et al. (2011). Geophysical features and hydrocarbon exploration prospecting of reef in Xisha offshore. *Prog. Geophys* 26 (5), 1771–1778. doi:10.3969/j.issn.1004-2903
- Yang, Z., Wu, S. G., Lv, F. L., Wang, D. W., Wang, B., and Lu, Y. T. (2014). Evolutionary model and control factors of late Cenozoic carbonate platform in Xisha area. *Mar. Geol. Quat. Geol.* 34 (5), 47–55.
- Yang, Z., Zhang, G. X., Zhang, L., and Xia, B. (2016). Development and evolution of Neogene reef in Xisha Sea area and its controlling factors. *Pet. Exp. Geol.* 38 (6), 787–795.
- Yang, Z. L., Wang, B., Li, L., Li, D., Zhang, Y., and Sun, G. Z. (2020). Characteristics of pockmarks and their Genesis Zhongjian offshore area, South China Sea. *Mar. Geol. Front.* 36.
- Ye, J. L., Wei, J. G., Liang, J. Q., Lu, J., Lu, H., and Zhang, W. (2019). Complex gas hydrate system in a gas chimney, South China Sea. *Mar. Petroleum Geol.* 104, 29–39. doi:10.1016/j.marpetgeo.2019.03.023
- Ye, Y. C., Lai, X. H., Liu, D. J., and Tian, S. F. (2011). A preliminary study for hazard geology division in China Sea areas. *Chin. J. Geol. Hazard Control* 22 (4), 102–107.
- Zhang, B. K., Li, S. Z., Xia, Z., Ma, Y., Yu, S., and Wang, X. F. (2014a). Distribution of Cenozoic igneous rocks and its relation to submarine geological hazards in the deepwater area of the northern South China Sea. *Acta Oceanol. Sin.* 36 (11), 90–100.
- Zhang, Q., Wu, S. G., Lyu, F. L., Dong, D. D., Yan, Q. S., and Yang, Z. (2014b). The seismic characteristics and the distribution of the igneous rocks in the Northwestern slope of the south China Sea. *Geotect. Metallogenia* 38 (4), 919–938.
- Zhao, Q. (2010). *The sedimentary research about reef carbonatite in Xisha Islands waters*. Qingdao, China: Institute of Oceanology, Chinese Academy of Sciences, 1–158. [D].